A Study on the Stiffness of Solid And Hollow Section Brass

by

Vinod A/L Chandra Sayakaran

Dissertation submitted in partial fulfillment of

the requirements for the

Bachelor of Engineering (Hons)

(Mechanical Engineering)

JULY 2010

Unversiti Teknologi PETRONAS

Bandar Seri Iskandar

31750 Tronoh

Perak Darul Ridzuan

CERTIFICATION OF APPROVAL

A Study on the Stiffness of Solid and Hollow Section Brass

by

Vinod A/L Chandra Sayakaran

A project dissertation submitted to the

Mechanical Engineering Programme

Universiti Teknologi PETRONAS

In partial fulfilment of the requirement for the

BACHELOR OF ENGINEERING (Hons)

(MECHANICAL ENGINEERING)

Approved by,

_____

(AP. DR. OTHMAN MAMAT)

UNVERSITI TEKNOLOGI PETRONAS

TRONOH, PERAK

JULY 2010

CERTIFICATION OF ORIGINALITY

This is to certify that I am responsible for the work submitted in this project, that the original work is my own except as specified in the references and acknowledgements, and that the original work contained herein have not been undertaken or done by unspecified sources or persons.

_____

(VINOD A/L CHANDRA SAYAKARAN)

ABSTRACT

Brass is an alloy of copper and zinc, with varieties of proportion yielding different types of brasses. Alpha brass is a high purity cold forming brass used in handrails, grillwork and radiator cores, with excellent suitability for brazing, soldering and cold-working. This project aimed to study the differences in stiffness of solid and hollow section brass components. A three-point bending test was performed to evaluate the stiffness of brass specimens, after which the specimen was fractured and examined using a Scanning Electron Microscope (SEM). The specimens were 6mm square sections with a span of 120mm, where the hollow specimen had a 4mm-diameter hole in the middle. Upon testing, the solid specimen yielded a stiffness of 729 kN/mm, which was greater than the 327 kN/mm value obtained from the hollow specimen. This proved theoretical expectations for solid specimen to have greater stiffness than hollow ones. SEM imaging results showed more pores in the solid specimen compared to the hollow specimen, but did not yield any significant differences in the microstructure of solid and hollow section brass upon fracture.

ACKNOWLEDGEMENTS

First and foremost I would like to thank God for His wondrous provision and blessings, the wisdom He gave to understand this topic and His love that never failed throughout the course of this project. Without God's hand that goes before me and His special favor, it would have never been possible to complete this report in the stipulated time.

Next, I would like to thank my parents and my aunt, who have continually given me monetary and moral support in order for me to keep focus in completing this project successfully. I also wish to express my utmost gratitude to AP Dr. Othman Mamat, my Supervisor, who took me in under his wings and placed his faith in me to complete this project despite the encompassing circumstances. Without his support and grace the project would not have been successful.

Fourthly, I would like to extend my gratitude toward Mr Mebrahitom, a PhD student in the Mechanical Engineering Department who has provided hands-on guidance on what was required to complete this report, and the understanding of terms related. Next, I wish to express my appreciation of the technicians in the Materials Engineering Lab, who were very cooperative in my lab work. Also, Mr Michael Low of Goldfarm Enterprise who helped me get my brass specimens at a lower price and prefabricated them for me. I am also grateful toward AP Dr. Nasir Shafiq and Mr Johan from the Civil Engineering Department who allowed me to use their lab facility.

Last but not least, I would like to acknowledge my friend, Taha Nasir, who has been a constant support and source of wisdom throughout the course of this project. With him and the friends around me, this project has been a joy to complete.

TABLE OF CONTENT

LIST OF FIGURE

LIST OF TABLES

CHAPTER 1
INTRODUCTION

1.1 Background of Study

The stiffness is defined as load required for a unit elastic deflection and is dependent on both the properties of the material from which it is made and the geometry of the structure (Hertzberg, 1996). In other words, stiffness is the ability of a material to maintain its shape when a load is acted upon it (Charles, Crane, & Furness, 1997). It is usually concerned with the relationship between stress and strain.

Stiffness is a very important property in the study of materials. It influences the choice of materials for certain applications. There are three reasons why stiffness is an important study in choice of a material. One of the concerns is with stable deflection; another is with the absorption of energy and the third, with failure by instability.

1. Deflection increases with the decrease of stiffness (Tiwari, 1997). Deflection is the displacement of a structural element under load (Kaushish, 2008). Therefore, less stiffness increases the instability of deflection. This is an important feature, because for example, in 1940, inadequate torsion stiffness in the bridge deck caused the collapse of the Tacoma Narrows Bridge (Robert G. Fuller, 2000).
2. Knowing a material's energy absorption helps to estimate effect to structures caused by collisions or any outward forces (X. Huanga, 2002). It gives an overall glimpse of how much strain a structure can withstand or the extent of deflection it can go before breaking.
3. Too stiff a material may make the material brittle, but the wrong range of stiffness may also cause failure with instability, where shape of structure is too flexible and too much change happen under strain or other factors (Bayer Corporation, 1995).

The stiffness of brass will be evaluated in this project. Brass is an alloy of copper and zinc, with varieties of proportion that gives range of different brasses. The type of brass used in this project is the alpha brass, also known as the American brass.

Alpha brass is a high purity cold forming brass. It is used when severe bending or riveting properties are required. It can be machined but only with slow speeds and very light feeds.

The many applications of alpha brass includes handrails and grillwork in architecture, tanks and radiator cores in automotive, socket shells and screw shells in electrical, bead chains and springs in industrials plus other areas such as builders hardware, fasteners, marine and plumbing.

In terms of fabrication, alpha brass has excellent suitability for brazing, soldering and high capacity for being cold-worked. Besides, it is also suitable for butt weld, oxyacetylene welding and spot weld. User should take note, however, that alpha brass has low capacity of being hot formed, and is not that suitable for coated metal arc welding and seam weld.

1.2 Problem Statement

This project intends to conduct a study to investigate the stiffness in bending for brass alloy, having different geometry. The criterion used is square beams of solid and hollow-type sections.

Experiments will be done to solve the unknown of brass's practical bending stiffness in comparison to those figures given theoretically. It is always important to test the validity or accuracy of material specification given by the industry. Often, standard specification or materials might have been done through studies by groups of people in countries different than ours, where factors like difference in atmosphere dampness, weather temperature and other environmental influence may not have been considered.

Therefore, material specifications such as bending stiffness given might differ from standard ones or those calculated theoretically, and research is done to fine out the exact reality ones.

1.3 Objective and Scope of Study

This project intends to evaluate and differentiate the stiffness of solid and hollow brass components. The project employs three-point bending test as means of obtaining the stiffness of the material. For this study, the scope is limited to square beams of solid section and square beams with circular hollow section.

CHAPTER 2
LITERATURE REVIEW/THEORY

2.1 Brass alloy and its properties

Brasses are copper-zinc alloys, commonly used in engineering applications due to their strength, corrosion resistance, appearance and colour, and ease of working and joining. This comes from the addition of zinc to copper that raises its strength and gives the additional properties. There are many types of brass, dependent on the composition and varying additives included (Illuminating Engineering Society, 1967).

Brasses are divided into two classes. The alpha alloys, with less than 37% zinc, and the alpha/beta alloys with 37-45% zinc. Alpha alloys are ductile and can be cold worked. Alpha/beta or duplex alloys have limited cold ductility and are harder and stronger (Alavdeen, Venkateshwaran, & Jappes, 2006).

The type of brass used in this study is alpha brass, with properties as shown in Table 5.1.

Table 2.1: Properties of Alpha Brass Alloys (Alavdeen, Venkateshwaran, & Jappes, 2006)

Density (g/cm^3)	Young's modulus (GPa)	Yield strength (MPa)	Ultimate Strength (GPa)
8.47	97	110	330

2.2 Stiffness

Stiffness can be defined as a measure of the resistance offered by an elastic body to deformation. (Kaushish, 2008) It is a property of a structure, dependent on the material, shape and boundary conditions (Sharpe, 2008).

The Young's modulus (E), commonly referred to as the elastic modulus, is the intrinsic property of the material that describes its tendency to deform along an axis

when opposing forces are applied along that axis. It is also defined as the ratio of tensile stress to tensile strain (Callister, 2007).

2.3 Ductility of materials

Ductility is a mechanical property that describes the extent in which solid materials can be plastically deformed without fracture (Kaushish, 2008). In materials science, ductility specifically refers to a material's ability to deform under tensile stress. This means how much it is permitted it to be reduced in cross sectional area without fracture. In a tensile test, ductile material show considerable elongation eventually failing by necking, with consequent rapid increase in local stresses. Therefore, a material’s ductility is very much dependent on its tensile strength and elasticity (Pradelle, 2007).

2.4 Transgranular fracture mechanism

Transgranular fracture is a fracture that follows the edges of lattices in a granular material, neglecting the grains in the individual lattices. These fracture paths proceed through metal grains rather than around the edge of metal grains. The transgranular fracture path can be ductile or brittle. If transgranular fracture is brittle a fracture pattern called cleavage will be displayed. (Janssen, Zuidema, & Wanhill, 2004)

This project will see involvement of transgranular cleavage fracture that denotes an inability to absorb impact energy. Cleavage is basically a fracture mechanism that is found in stronger metal and occurs at lower temperatures. (Pradelle, 2007) Cleavage is usually associated or found when failure occurs at high rates of energy input, which includes how this study will be conducted, giving strain and load to the alpha brass till the point of fracture.

2.5 Intergranular fracture mechanism

Intergranular fracture is decohesion that may occur along a weakened grain boundary. It is the crack traveling along the grain boundaries, and not through the actual grains. Fracture normally changes direction to follow the new grain. This will results in a fairly jagged looking fracture with Straight, bumpy edges of the grain and

shiny surface. Intergranular fracture usually occurs when the phase in the grain boundary is weak and brittle. (Janssen, Zuidema, & Wanhill, 2004)

One of the main causes of intergranular fracture is cyclic loading when the material has insufficient number of independent slip systems to accommodate plastic deformation between contiguous grains leading to grain boundaries (Janssen, Zuidema, & Wanhill, 2004). Therefore, this is another type of fracture this study will observe.

2.6 Porosity (Pores) in materials

Porosity is a measure of the void spaces in a material. It can be defined as fraction of the volume of voids over the total volume, between 0–1, or as a percentage between 0–100 percent. Porosity represents the storage capacity, influenced by the spaces between the grains that make up that material. The more tightly packed the grains are, the lower the porosity (Brandon & Kaplan, 2008).

It is important to know the porosity of one material. Porosity in materials greatly reduces the strength and load carrying characteristics of the material. Porosity is usually determined by the shape of the grains and the range of grain sizes present, how they are arranged and if void between larger grains are filled with the smaller grains (Cramer & Sevostianov, 2009). Therefore, grain size of two materials (copper and zinc) in an alloy (alpha brass) determines its porosity. If the grains fall in place and fit nicely, porosity will be lower.

2.7 Bending test of materials

Various bending and torsion tests are widely used for evaluating the elastic modulus, strength, shear modulus, shear strength and other properties of materials. These tests differ in a critical way from tension and compression tests, in that the stresses and strains are not uniform over the cross-section of the test specimen.

2.7.1 Three-point Bend Test

The specimens often have rectangular cross sections and may be loaded in either three-point bending or four-point bending, as shown in Figure 2.1.

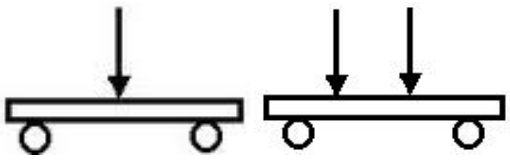

(a) (b)

Figure 2.1: Loading configuration for (a) 3-point bending and (b) 4-point bending

In bending, it is noted that the stress varies through the depth of the beam in such a way that yielding first occurs in a thin surface layer. This results in the load versus deflection curve not being sensitive to the very beginning of yielding. Also, if the stress-strain curve is not linear, as after yielding, the simple elastic bending analysis is not valid. (Meyers & Chawla, 2009)

The Second moment of area, I_x, is an important property in the three-point bend test.

1. Solid specimen

$$I_x = \frac{bh^3}{12} \qquad \text{(Eq. 1)}$$

2. Hollow specimen

$$I_x = \frac{bh^3}{12} - \frac{\pi r^4}{4} \qquad \text{(Eq. 2)}$$

Where

b = breadth of the specimen (m)

h = height of the specimen (m)

r = radius of the internal hole of the hollow section (m)

Theoretical value of central deflection, δ, for the specimen upon a given load is given by:

$$\delta = \frac{WL^3}{48EI_x} \qquad \text{(Eq. 3)}$$

Where

W = central load in Newton (g= 9.81 m/s^2)
L = distance between roller supports (m)
E = Young's modulus in material (N/m^2)
I_x = second moment of area of the beam (m^4)
(Meyers & Chawla, 2009)

T. Tiwari noted a clear variation of flexural strength for various sizes of specimen used in the bend test. For square and rectangular cross-sectional specimens, the decrease in dimension yields a greater measured flexural strength. Also discovered is the difference of flexural strength depending on the volume of material under tension. In the 4-point bending test, the volume of material below the neutral axis is under maximum tensile stress and is where failure will be initiated.

The behavior of the material exhibits near-perfect brittleness, with instantaneous crack propagation. Thus, the crack initiation is the critical step in flexural testing of such materials (Tiwari, 1997).

2.8 Scanning Electron Microscope

The Scanning Electron Microscope (SEM) consists of a source of high energy electrons and condenser system but with a probe which focuses the electron beam on to the specimen (Brandon & Kaplan, 2008). The probe lens is placed above the specimen as shown in figure.

As SEM uses electron beams, the collision of the electron that occurs with the specimen creates an elastic scattering. Thus, an energy loss occurs as the atomic

activity increases with the excitement of atoms (Abbaschian, Abbaschian, & Reed-Hill, 2009).

The ‘image’ to be captured is obtained by scanning the electron probe over the specimen surface in a television raster. From there an image signal is captured, processed and amplified accordingly and thus displayed in a monitor. In SEM the information is collected sequentially for each data point in turn. To obtain a well formed image, the scanning speed is restricted so that all the image points on the specimen are recorded (Brandon & Kaplan, 2008).

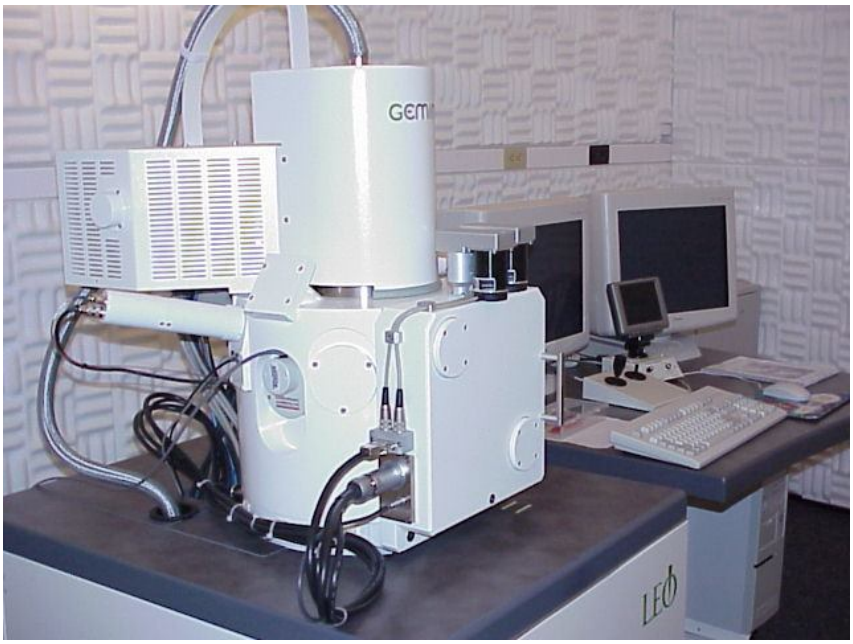

Figure 2.2 Scanning Electron Microscope

CHAPTER 3
METHODOLOGY

3.1 Experimental techniques

The following experimental techniques were used to obtain data in this project.

3.1.1 Three-point Bend Test

The specimens are to be tested under a three-point loading condition using the Three-Point Bending Apparatus located in the Materials Lab in Building 17 of UTP.

1. First, measurements are taken of the specimen and the distance between loading supports of the apparatus. Using Equations (1) and (2) the corresponding second moment of area, I_x is calculated. With that, and using Equation (3) the theoretical central deflection for load increments of 0.2kg until the maximum load available is calculated.
2. As the centre-loading weight is raised, the solid specimen sample is placed on the support of the apparatus, making sure that the centre point of the apparatus meets the centre point of the specimen. The minimal pre-loading is rested on the specimen, and the deflection gage is reset to zero.
3. The first loading of 0.2kg (1.962N) is placed on the specimen, and the deflection recorded is taken. The placement of the weight is done with extreme care, due to the very sensitive nature of the deflection gage. This step is repeated for every increment of 0.2kg, until the maximum load is met.
4. The weights are all removed, and the specimen is carefully taken out.
5. Steps (4) and (5) are repeated for the hollow specimen.
6. Data is tabulated and graphs of deflection (mm) versus load (kg) are plotted for each specimen.
7. From each graph the slope that corresponds to the stiffness (N/mm) is obtained.
8. The Young's modulus, E for each specimen is computed and compared with the theoretical value.

3.1.2 Preparation of specimen

The specimen was prepared in accordance with the Scanning Electron Microscope specifications and standards. Due to the thickness of the original beam, it was noted that to fracture the beam itself would require a very heavy load. The unavailability of such a load demanded the beam to be milled to a smaller specification. All four sides were milled off by 1 mm so that the resultant beam size would be 6 mm by 6 mm.

The resized beam was then to be fractured, so the concept of impact testing was used. Under impact testing, there is a method known as drop-weight test where the ductile-brittle transition is determined. Making use of the drop-weight concept at room temperature, as shown in Figure 3.1, both the beams, hollow and solid, were fractured. The beams were then taken to be analyzed under the Scanning Electron Microscope.

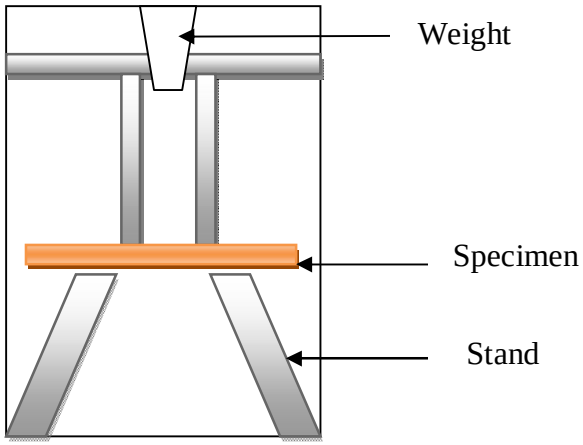

Figure 3.1: Drop Weight Technique

3.1.3 Microscopy using Scanning Electron Microscope

The sides containing fractured surfaces of the specimen were cut out from the beam using a mechanical cutter to a length of between 0.5cm and 2cm, to fit into the specimen holder of the microscope. The samples were then sent for sample preparation, where they are prepared for the high-vacuum imaging environment.

The dry samples are mounted onto the specimen holder and inserted into the microscope. Procedures for magnification onto the samples are done by trained lab technicians, who are guided on the areas requiring images and the magnification amount.

3.1.4 Analysis of Microscopic Images

The images captured from the microscopy were then analyzed. The comparison made was between the differences in microstructure of hollow and solid specimens.

3.2 Gantt Chart of the project

The following chart shows the activities planned for the FYP 2.

No	Detail/Week	1	2	3	4	5	6		7	8	9	10	11	12	13	14	14+
1	Project work continues	▬	▬	▬													
2	Submission of Progress Report 1				▲												
3	Project work continues				▬	▬	▬										
4	Submission of Progress Report 2									▲							
5	Seminar									▲							
6	Project work continues								▬	▬	▬	▬	▬	▬	▬	▬	▬
7	Poster Exhibition												▲				
8	Submission of Dissertation Final Draft															▲	
9	Oral Presentation																▲
10	Submission of Dissertation (hard bound)																▲

▲ Key Milestone ▬ Process

CHAPTER 4
ANALYSIS OF MICROSTRUCTURES

The beams, after fracture, were viewed under the Scanning Electron Microscope with various magnifications; 30 X, 100 X, 500X, 1000X and 2000 X. The analysis of the microstructure was to find out the following; ductility, transgranular and intergranular fractures and pores at the grain boundaries and within the grains itself. The analysis follows below.

4.1 Analysis of the Microstructure of Solid Brass Specimen

The fractured area of the solid specimen is zoomed in to observe how the microstructure is. Figure 4.1 shows a magnification of 30X. However, in order to give a better observation the specimen has to be further magnified.

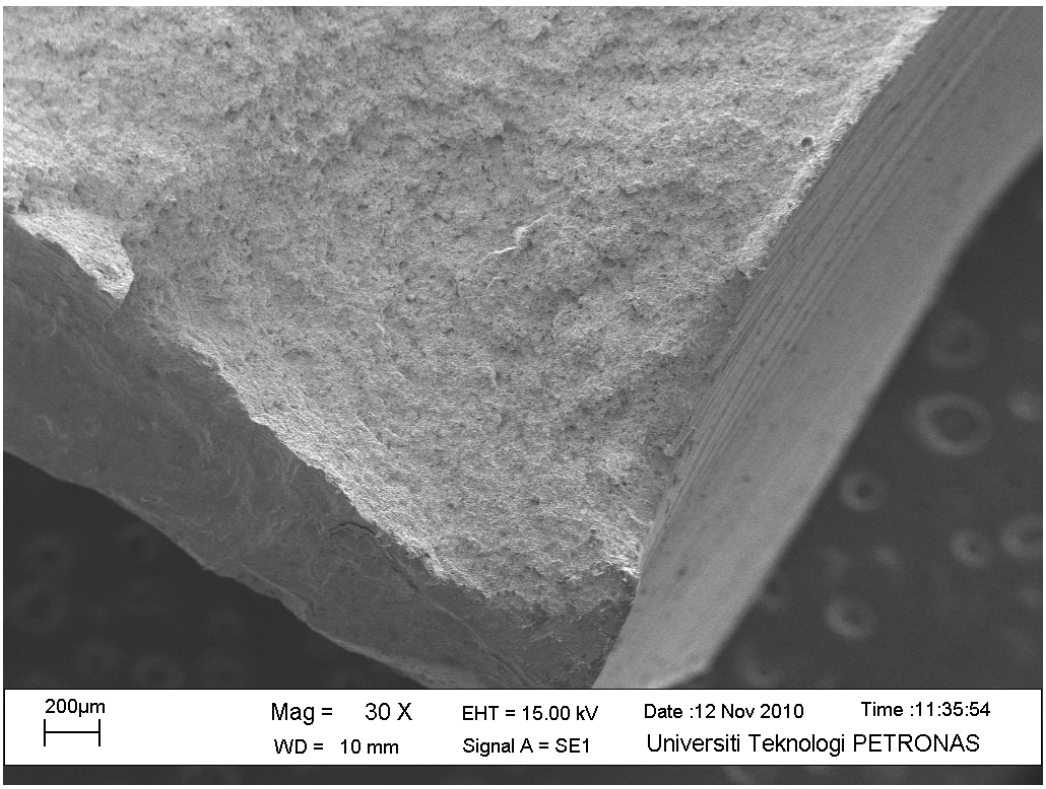

Figure 4.1: Micrograph of the fractured area at a magnification of 30 X

The solid specimen area observed in Figure 4.1 is magnified to a magnification of 100X. The fracture of the specimen is considered to be plastic due to the deformation at the edge of the specimen as shown (circled) in Figure 4.2.

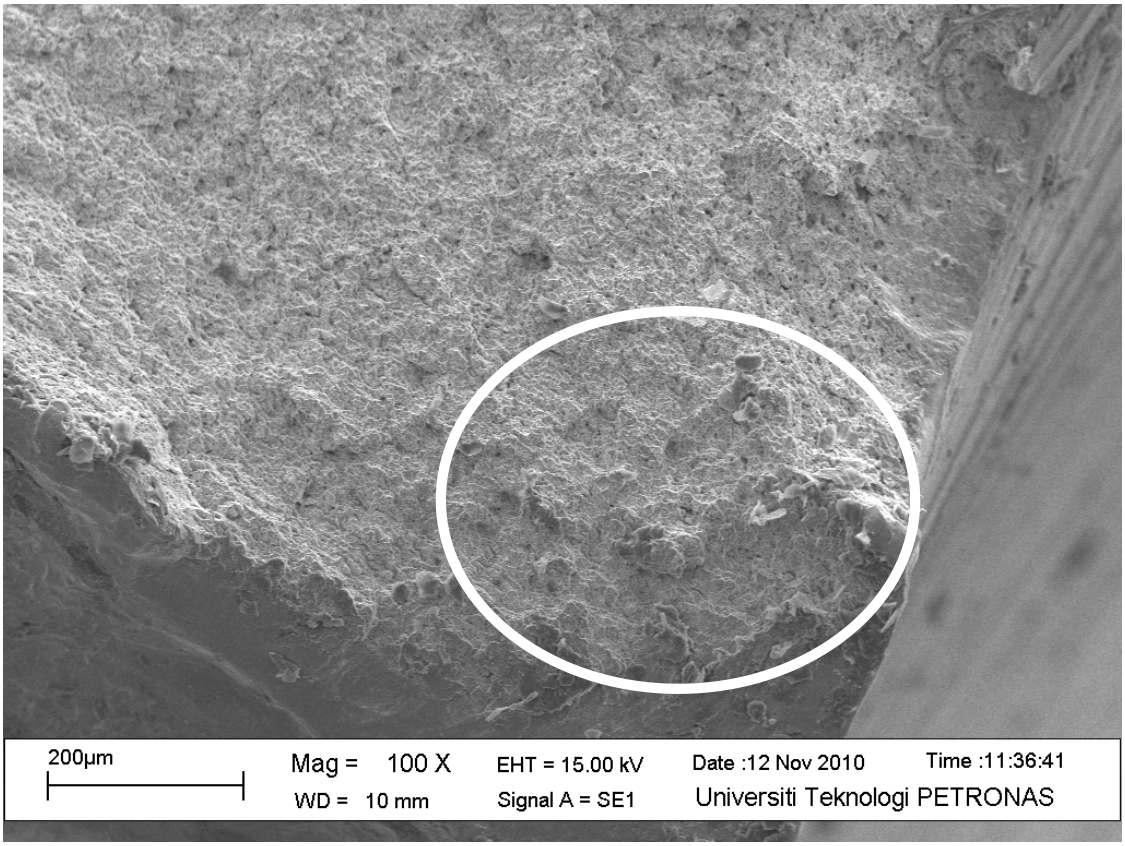

Figure 4.2: Micrograph of the fractured area at a magnification of 100 X

The same area observed in Figure 4.2 is further magnified, to a magnification of 500X, as shown in Figure 4.3. The circled area displays a very interesting feature. As observed in the rest of the micrographs, most of the fractures are transgranular, this on the other hand is intergranular on the same surface. Towards the left side of the micrograph transgranular fracture is observed.

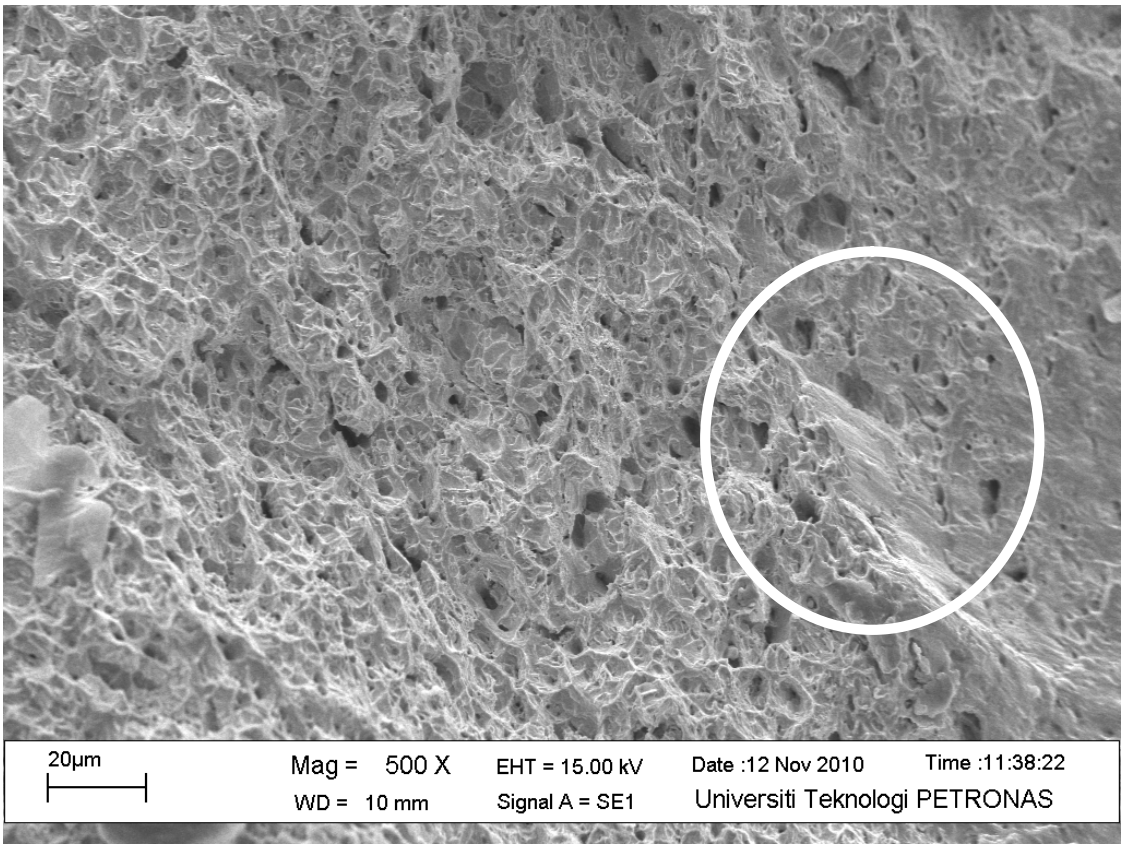

Figure 4.3: Micrograph of the fractured area at a magnification of 500 X

The fractured specimen area observed in Figure 4.3 is further magnified to 1000X magnification to observe for pores, as shown in Figure 4.4 (circled).

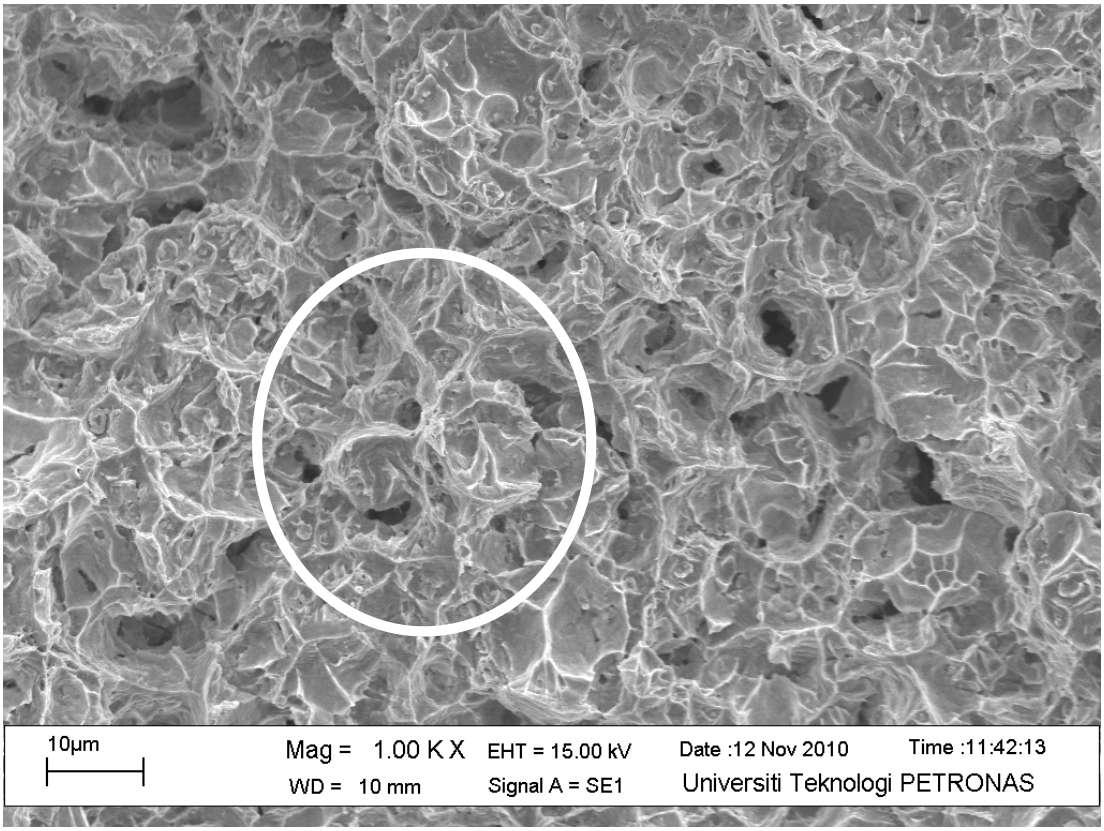

Figure 4.4: Micrograph of the fractured area at a magnification of 1000 X

The fractured specimen is magnified further, to 2000X magnification. Evidence of a transgranular fracture is observed as shown in Figure 4.5(circled), as the fracture passes through the grains.

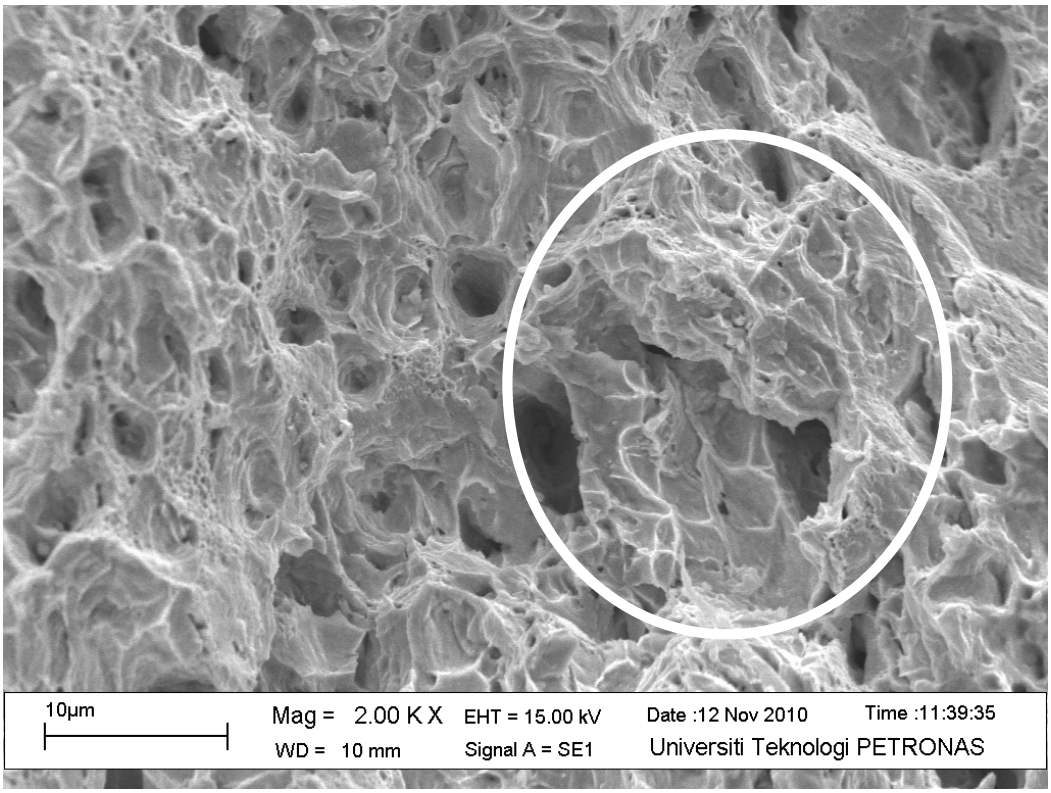

Figure 4.5: Micrograph of the fractured area at a magnification of 2000 X

4.2 Analysis of the Microstructure of Hollow Brass Specimen

The fractured area of the hollow specimen is magnified to observe its microstructure. The edge of the fractured specimen is zoomed in to a magnification of 30X, where two regions of different fractured surface is observed, as shown in Figure 4.6 (circled).

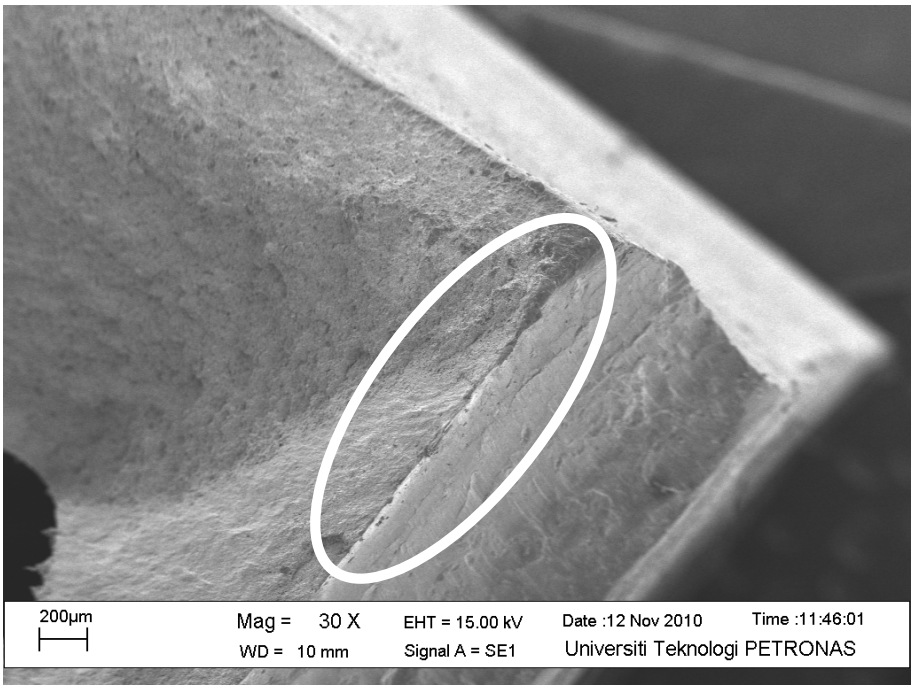

Figure 4.6: Micrograph of the fractured area at a magnification of 30 X

The region of differing fracture surface type is further magnified, to a magnification of 100X, and the differences are more obvious as shown in Figure 4.7. The arrows indicate each region.

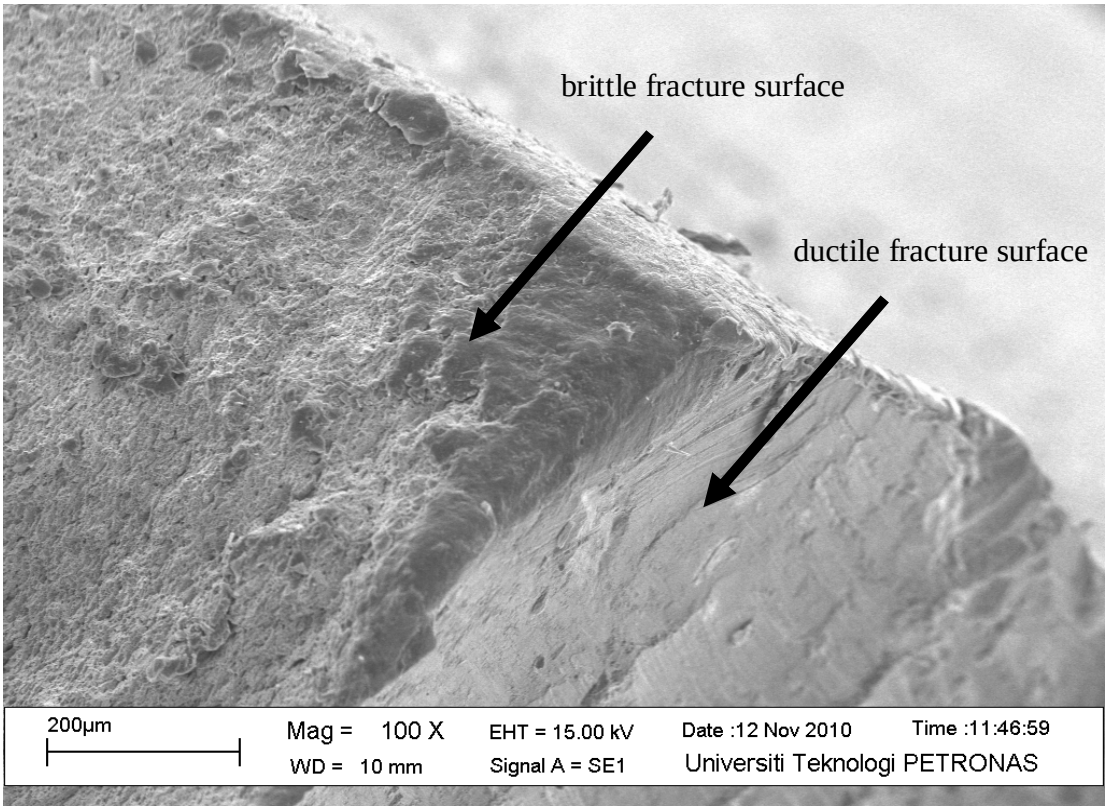

Figure 4.7: Micrograph of the fractured area at a magnification of 100 X

The fractured surface close to the hollow section of the specimen is magnified to a magnification of 100X, as shown in Figure 4.8. Brittle fracture is observed in this region, but fracture modes are unclear. Two sections of the fracture surface are further magnified (circled areas), as shown in Figures 4.9 and 4.10.

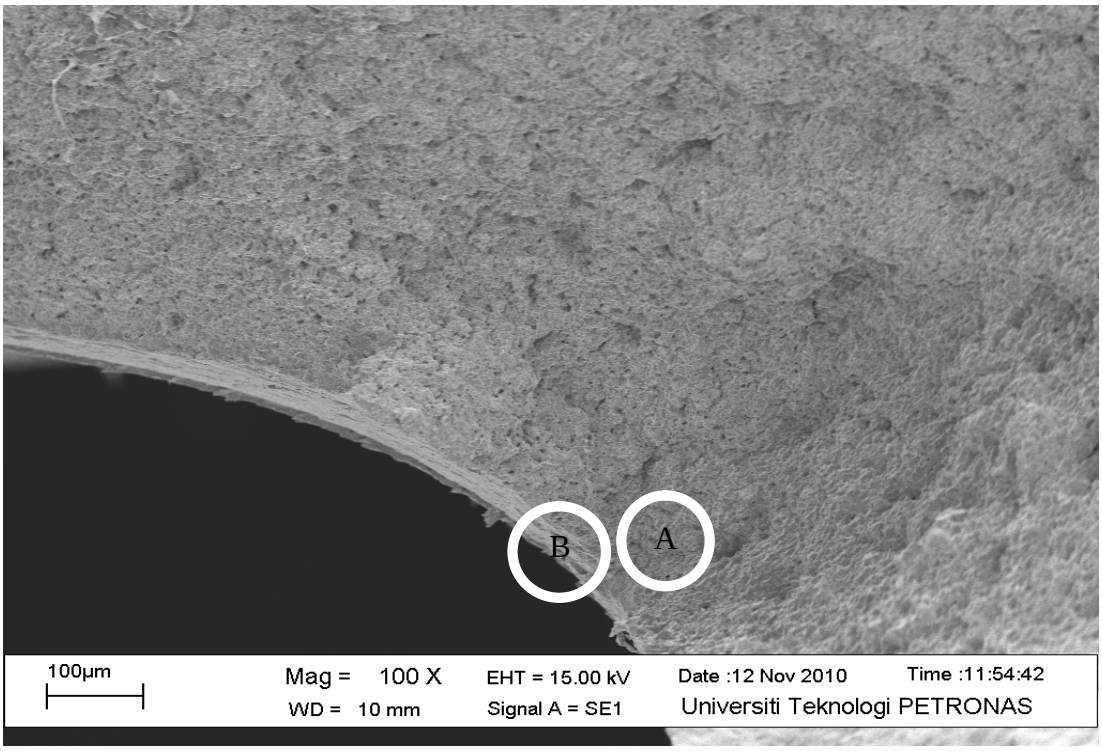

Figure 4.8: Micrograph of the fractured area at the edge of the hollow tube at a magnification of 100 X

The encircled area A near the hollow section of the specimen observed in Figure 4.8 is further magnified to a magnification of 500X, as shown in Figure 4.9.

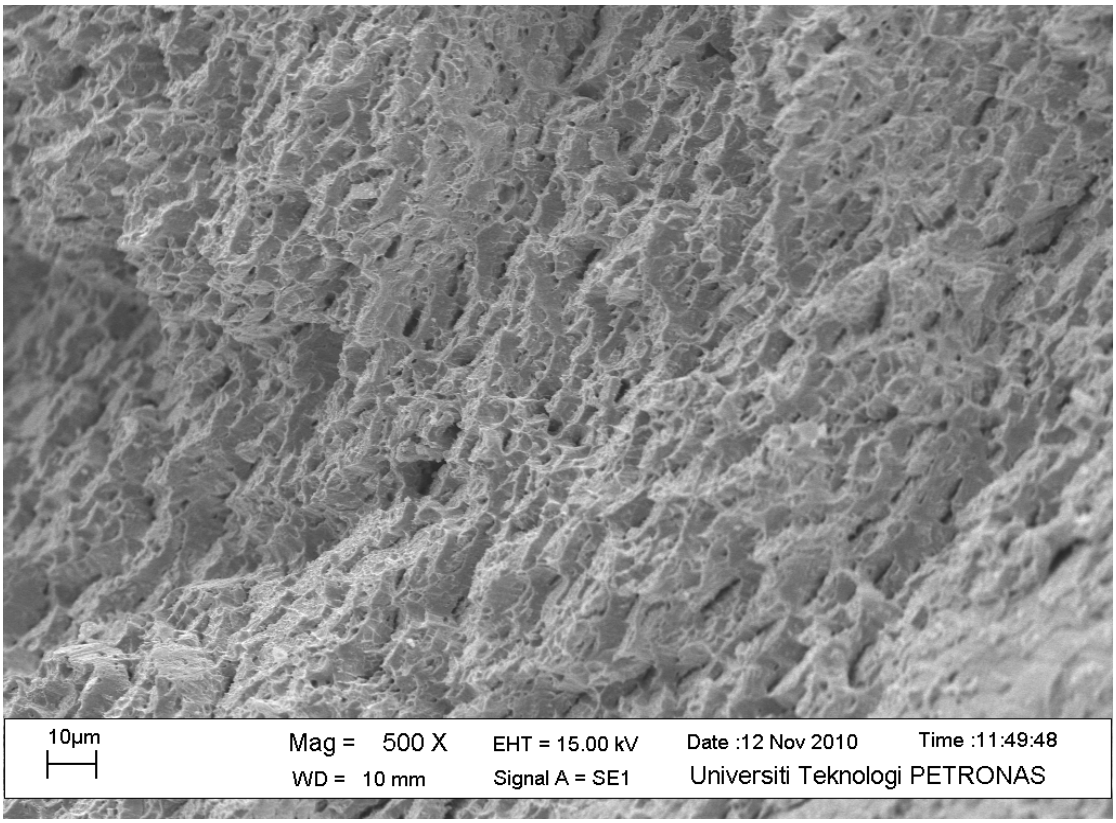

Figure 4.9: Micrograph of the fractured area at a magnification of 500 X

The encircled area B near the hollow section of the specimen observed in Figure 4.8 is further magnified to a magnification of 500X, as shown in Figure 4.10. Fracture mode in this region is not identifiable as magnification is unclear.

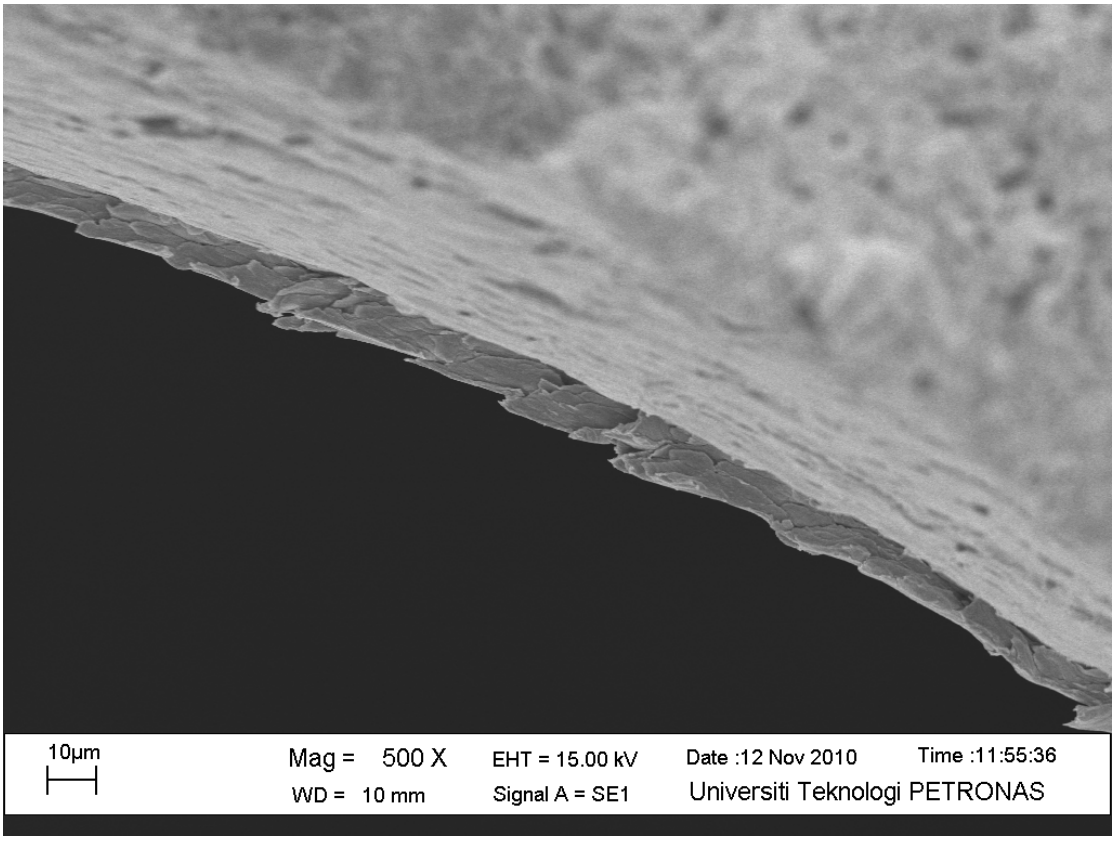

Figure 4.10: Micrograph of the fractured area at the hollow tube at a magnification of 500 X

The fractured region A observed from Figures 4.8 and 4.9 is further magnified to a magnification of 2000X, and pores are observed, as shown in Figure 4.11.

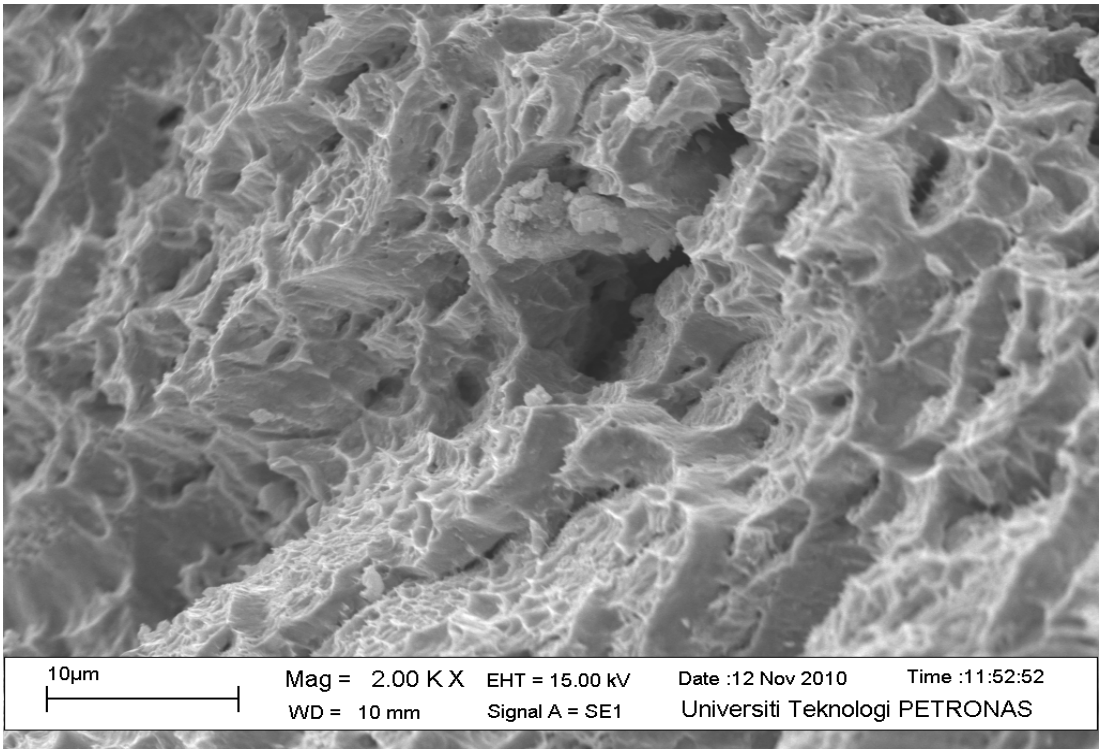

Figure 4.11: Micrograph of the fractured area at a magnification of 2000 X

The fractured region B observed from Figures 4.8 and 4.10 is further magnified to a magnification of 2000X, and jagged edges are observed, as shown in Figure 4.12.

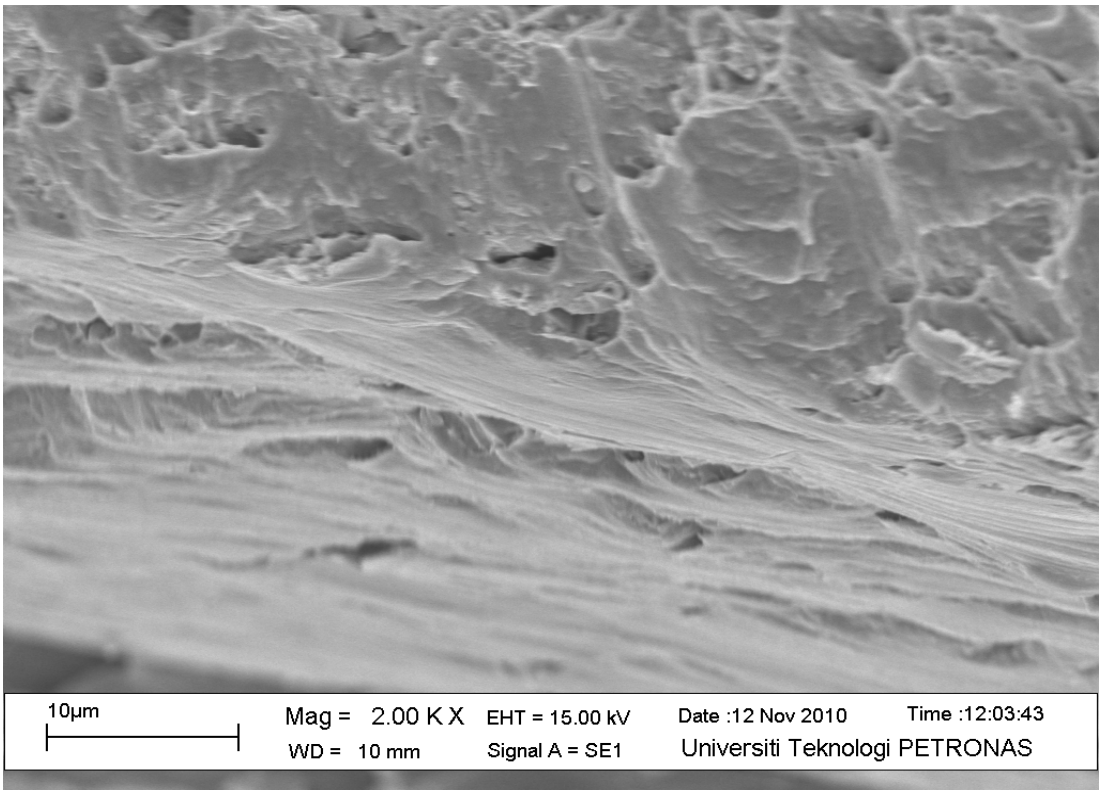

Figure 4.12: Micrograph of the fractured area at the hollow tube at a magnification of 2000 X

Ultimately, the fracture mode observation for the hollow specimen is inconclusive, but it is noted that not many pores were seen compared to the solid specimen.

CHAPTER 5
RESULTS AND DISCUSSION

5.1 Results from 3-point Bending Test

5.1.1 Theoretical results of deflection

The theoretical deflection is obtained from Equation (3).

$$\delta = \frac{WL^3}{48EI_x}$$

Theoretically calculated values of the deflection of the solid specimen based on Equation (3) are shown in Table 5.1.

Table 5.1 Theoretical deflection of solid specimen

Load, W (N)	Theoretical deflection, (m)
1.962	0.0000037
3.924	0.0000073
5.886	0.0000147
7.848	0.0000196
9.81	0.0000245
11.772	0.0000293
13.734	0.0000342
15.696	0.0000391
17.648	0.0000440
19.62	0.0000489
21.582	0.0000538
23.544	0.0000587
25.506	0.0000636
27.468	0.0000685
29.43	0.0000734

An example of the calculation of theoretical deflection for solid section with load of 1.962 N is as follows:

$$\delta = \frac{WL^3}{48EI_x}$$

$$\delta = \frac{1.962 \times 0.1^3}{48 \times (103 \times 10^9)(1.0800 \times 10^{-10})}$$

$$\delta = 0.0000037$$

Theoretically calculated values of the deflection of the hollow specimen based on Equation (3) are shown in Table 5.2.

Table 5.2 Theoretical deflection of hollow specimen

Load, W (N)	Theoretical deflection, (m)
1.962	0.0000055
3.924	0.0000111
5.886	0.0000166
7.848	0.0000221
9.81	0.0000277
11.772	0.0000332
13.734	0.0000387
15.696	0.0000443
17.648	0.0000498
19.62	0.0000553
21.582	0.0000609
23.544	0.0000664
25.506	0.0000720
27.468	0.0000775
29.43	0.0000830

5.1.2 Experimental results of deflection

Experimentally obtained values of the deflection of the solid specimen are shown in Table 5.3.

Table 5.3 Experimental deflection of solid specimen

Experimental Deflection (m)	Load (N)
0.000005	1.962
0.000012	3.924
0.000015	5.886
0.000020	7.848
0.000025	9.810
0.000030	11.772
0.000035	13.734
0.000042	15.696
0.000048	17.648
0.000054	19.620
0.000058	21.582
0.000064	23.544
0.000070	25.506
0.000075	27.468
0.000080	29.430
0.000095	35.316

Experimentally obtained values of the deflection of the hollow specimen are shown in Table 5.4.

Table 5.4 Experimental deflection of hollow specimen

Experimental Deflection (m)	Load (N)
0.000006	1.962
0.000012	3.924
0.000018	5.886
0.000024	7.848
0.000030	9.810
0.000036	11.772
0.000042	13.734
0.000048	15.696
0.000054	17.648
0.000060	19.620
0.000066	21.582
0.000072	23.544
0.000078	25.506
0.000084	27.468
0.000090	29.430
0.000108	35.316

A graph of Load versus Experimental Deflection of specimen is plotted for both specimens, as shown in Figure 5.5, to compare the slope (which corresponds to the stiffness of the specimen) and then further to calculate the experimental value of the Young's modulus, E.

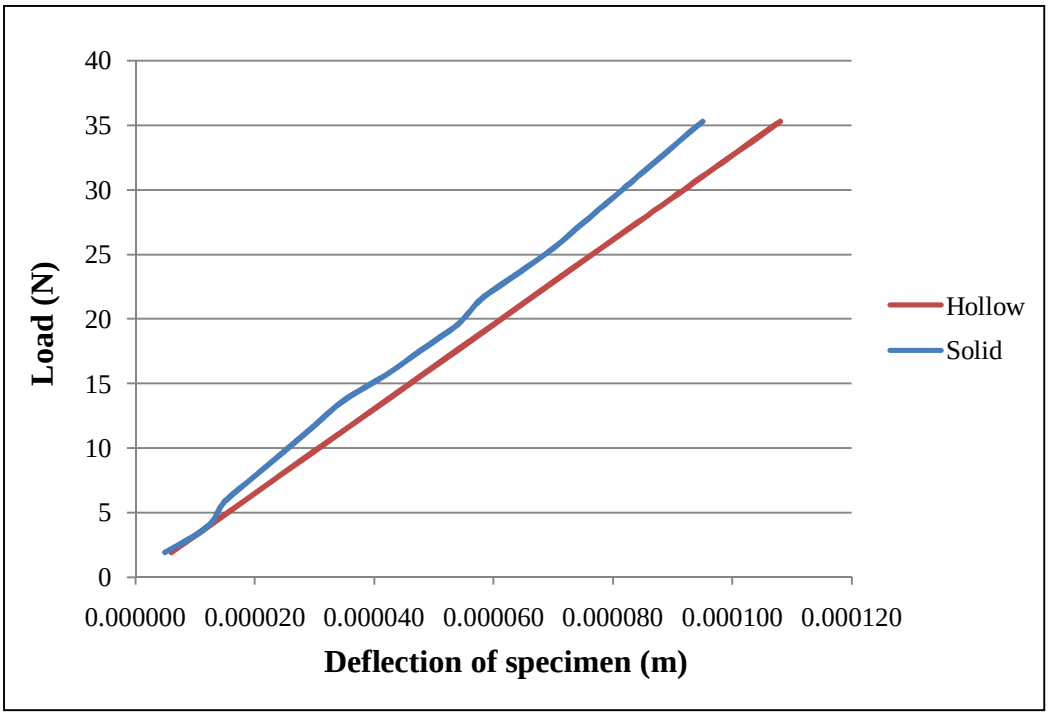

Figure 5.1 Graph of Load versus Experimental Deflection of solid and hollow specimen

The slope of the graph from data corresponds to the stiffness, k = W/∂ (N/mm). From the stiffness obtained, the second moment of area is calculated using Equations (1) and (2).

Using Equation (1):

$$I_x = \frac{bh^3}{12}$$

$$I_x = \frac{(0.006)(0.006)^3}{12}$$

$$I_x = 1.0800 \times 10^{-10}$$

Using Equation (2):

$$I_x = \frac{bh^3}{12} - \frac{\pi r^4}{4}$$

$$I_x = \frac{(0.006)(0.006)^3}{12} - \frac{\pi(0.0015)^4}{4}$$

$$I_x = 9.5434 \times 10^{-11}$$

Table 5.5: Stiffness from graph and Second Moment of Area calculated

Specimen	Stiffness, k (kN/mm)	Second moment of area of beam, $I_x \left(m^4\right)$
Solid	729	1.0800×10^{-10}
Hollow	327	9.5434×10^{-11}

The theoretical value of Young's modulus (E) is calculated using Equation (4),

$$E = \frac{kL^3}{48I_x}$$

Where:

L – span (m)

k – from slope of graph, corresponds to the stiffness (N/mm)

I_x - second moment of area of beam (m^4)

For the 6mm solid specimen, the value of E obtained is shown below.

$$E = \frac{kL^3}{48I_x}$$

$$E = 80.826 GPa$$

The percentage of error from the theoretical value of 79GPa is 2.3%.

For the 6mm hollow specimen, the value of E obtained is shown below.

$$E = \frac{kL^3}{48I_x}$$

$$E = 81.393 GPa$$

The percentage of error from the theoretical value of 79GPa is 3.7%.

It is noted that for both solid and hollow specimens, there is a percentage of error in the value of the Young's modulus calculated from experimental data when compared to the theoretical value. This is expected, and there are many reasons for which such differences in value occur. They may be due to parallax error in recording the deflection reading from the gage. Also to be noted, with the formulas used any minor difference in value recorded could result in a big difference due to multiplication to the power of 3 or 4. The gage itself may have some errors due to the preload or when the weights are being placed on it.

CHAPTER 6
CONCLUSION

In this research project, the three-point bending test was utilized successfully to evaluate the stiffness in bending of the solid and hollow section brass specimens. Results showed that the solid specimen had a stiffness of 729 kN/mm, and the hollow specimen had a stiffness of 327 kN/mm. This supports theoretical expectation for the solid specimen to possess greater stiffness. It is noted that the actual deflection for both solid and hollow specimens are greater than the theoretical expected value from calculations.

The Young's modulus was successfully calculated from the experimental data, with the solid specimen yielding a value of 80.826 GPa and the hollow specimen 81.893 GPa. With the allowance of errors of 2.3% and 3.7% respectively for solid and hollow specimens (when compared to the theoretical value of 79 GPa), it is proven that the Young's modulus is a constant value for a material irrespective of its geometry.

REFERENCES

1. Abbaschian, R., Abbaschian, L., & Reed-Hill, R. E. (2009). *Physical Metallurgy Principles.* Cengage Learning.

2. Alavdeen, A., Venkateshwaran, N., & Jappes, D. W. (2006). *A Textbook of Engineering Materials and Metallurgy.* New Delhi: Laxmi Publications (P) Limited.

3. Bailey, D. (1997). *Ductile Fracture.* Retrieved October 2010, from http://www.sv.vt.edu/classes/MSE2094_NoteBook/97ClassProj/exper/bailey/www/bailey.html

4. Ballard, J. (1997). *Brittle Fracture.* Retrieved November 2010, from http://www.sv.vt.edu/classes/MSE2094_NoteBook/97ClassProj/exper/ballard/www/ballard.html

5. Bayer Corporation. (1995). Engineering Polymers Material Selection. Bayer Corporation.

6. Brandon, D., & Kaplan, W. D. (2008). *Microstructural Characterization of Materials, 2nd Edition.* Wiley.

7. Budinski, M. K., & Budinski, K. G. (2010). *Engineering Materials, 9th Edition.* New Jersey: Pearson.

8. Callister, W. D. (2007). *Materials Science and Engineering: An Introduction, 7th Edition.* Wiley.

9. Charles, J. A., Crane, F. A., & Furness, J. A. (1997). *Selection and use of engineering materials.* Butterworth-Heinemann.

10. Cramer, M., & Sevostianov, I. (2009). Effect of Pore Distribution on Elastic Stiffness and Fracture Toughness of Porous Materials. *Letters in Fracture and Micromechanics, Springer Media* .

11. Hertzberg, R. W. (1996). *Deformation and Fracture Mechanics of Engineering Materials, 4th Edition.* Hoboken, NJ: John Wiley and Sons Inc.

12. Illuminating Engineering Society. (1967). *Illuminating engineering, Volume 62.* University of Minnesota: Illuminating Engineering Society.

13. Intertek Plastics Technology Laboratories. (2010). *Flexural Properties.* Retrieved November 2010, from Intertek Plastics Technology Laboratories: http://www.ptli.com/testlopedia/tests/Flex-D790.asp

14. Janssen, M., Zuidema, J., & Wanhill, R. (2004). *Fracture Mechanics.* New York: Taylor & Francis.

15. Kaushish, J. P. (2008). *Manufacturing Processes.* New Delhi: PHI Learning Pvt. Ltd.

16. Meyers, M., & Chawla, K. (2009). *Mechanical Behavior of Materials, 2nd Edition.* Cambridge University Press.

17. Pradelle, M. A. (2007, May 2). *A Brittle Fracture-Based Experimental Methodology For Ductile Damage Analysis.* Retrieved November 2010, from http://www.mate.tue.nl/mate/pdfs/8447.pdf

18. Professor William N. Sharpe, J. (2008). *Springer Handbook of Experimental Solid Mechanics.* Springer .

19. Robert G. Fuller, C. R. (2000). Twin Views of the Tacoma Narrows Bridge Collapse. USA: American Association of Physics Teachers.

20. Tiwari, R. (1997). Effect of Specimen Characteristics on Flexural Strength. 1-2.

21. University of Bristol School of Chemistry. (n.d.). *Scanning Electron Microscopy.* Retrieved 2010, from http://www.chm.bris.ac.uk/pt/diamond/stuthesis/chapter2.htm

22. X. Huanga, G. L. (2002). Energy absorption in splitting square metal tubes. *Science Direct* .